



Current estimates of K_1^* and K_2^* appear inconsistent with measured CO_2 system parameters in cold oceanic regions

Olivier Sulpis^{1,2}, Siv K. Lauvset³, Mathilde Hagens⁴

¹Department of Earth Sciences, Utrecht University, Utrecht, The Netherlands

5 ²Department of Earth and Planetary Sciences, McGill University, Montreal, Canada

³NORCE Norwegian Research Centre, Bjerknes Centre for Climate Research, Bergen, Norway

⁴Soil Chemistry and Chemical Soil Quality, Wageningen University and Research, Wageningen, The Netherlands

Correspondence to: Olivier Sulpis (o.j.t.sulpis@uu.nl)

Abstract. Seawater absorption of anthropogenic atmospheric carbon dioxide (CO_2) has led to a range of changes in carbonate chemistry, collectively referred to as ocean acidification. Stoichiometric dissociation constants used to convert measured carbonate system variables (pH, $p\text{CO}_2$, dissolved inorganic carbon, total alkalinity) into globally comparable parameters are crucial for accurately quantifying these changes. The temperature and salinity coefficients of these constants have generally been experimentally derived under controlled laboratory conditions. Here, we use field measurements of carbonate system variables taken from the Global Ocean Data Analysis Project version 2 and the Surface Ocean CO_2 Atlas databases to evaluate the temperature dependence of the carbonic acid stoichiometric dissociation constants. By applying a novel iterative procedure to a large dataset of 948 surface-water, quality-controlled samples where four carbonate system variables were independently measured, we show that the set of equations published by Lueker et al. (2000), currently preferred by the ocean acidification community, overestimates the stoichiometric dissociation constants at low temperatures, below $\sim 8^\circ\text{C}$. We apply these newly derived temperature coefficients to high-latitude Argo float and cruise data to quantify the effects on surface-water $p\text{CO}_2$ and calcite saturation states. These findings highlight the critical implications of uncertainty in stoichiometric dissociation constants for future projections of ocean acidification in polar regions, and the need to improve knowledge of what causes the CO_2 system inconsistencies in cold waters.

10
15
20

25



30 1 Introduction

In the last decades, oceans have absorbed over a quarter of the anthropogenic carbon dioxide (CO₂) emitted to the atmosphere (Le Quéré et al., 2018; Gruber et al., 2019). Upon dissolution in seawater, this CO₂ triggers a suite of reactions that lead to a range of chemical changes jointly termed ocean acidification (Zeebe and Wolf-Gladrow, 2001; Gattuso and Hansson, 2011). To accurately calculate the magnitude of these changes, it is crucial to understand the chemical behaviour of CO₂ in seawater.

Upon dissolution, CO₂ takes the form of solvated CO₂ (CO_{2(aq)}, CO₂·H₂O) or carbonic acid (H₂CO₃), which are here both represented by H₂CO₃^{*}, since they can only be readily distinguished by infra-red spectrometry (Zeebe and Wolf-Gladrow, 2001), and the following series of reactions occurs:



Together, these three reactions and their species constitute the marine CO₂-H₂O system, which is responsible for about 95% of the acid-base buffering capacity of seawater and maintains the pH of the ocean within a narrow range (Bates, 2019; Zeebe and Wolf-Gladrow, 2001).

At equilibrium, the ratio of the activities or effective concentrations of the reaction products to the product of reactant activities that appear in Eqs. (2) and (3) yields a constant that describes the thermodynamic equilibrium of these reactions. Eqs. (2) and (3) describe the first and second step in the dissociation of carbonic acid and are therefore termed the first and second dissociation constants, K₁ and K₂, respectively. To avoid the use of activity coefficients, which are not straightforward to derive in seawater, marine scientists have developed a set of *stoichiometric* (or apparent) equilibrium constants to represent the state of the system at a given pressure (*P*), temperature (*T*) and salinity (*S*). To describe the carbonate system, two stoichiometric constants (*K*₁^{*} and *K*₂^{*}, conventionally denoted by a star) are defined in terms of the concentrations of the different species:

$$55 \quad K_1^* = \frac{[\text{HCO}_3^-][\text{H}^+]}{[\text{H}_2\text{CO}_3^*]} \quad (4),$$

$$K_2^* = \frac{[\text{H}^+][\text{CO}_3^{2-}]}{[\text{HCO}_3^-]} \quad (5).$$

Using these stoichiometric equilibrium constants, we can calculate the relative quantities of the dissolved inorganic carbon (DIC = [H₂CO₃^{*}] + [HCO₃⁻] + [CO₃²⁻]) species. With improved analytical techniques, measurement accuracy of carbonate system variables has substantially increased over the past decades. As a result, uncertainty in carbonate system calculations is



currently dominated by the uncertainty of K_1^* and K_2^* values (Orr et al., 2018), justifying the need to investigate whether these uncertainties can be reduced.

Using popular software for carbonate system calculations, e.g., CO2SYS (Lewis and Wallace, 1998; Pierrot et al., 2006; van Heuven et al., 2011) or seacarb (Gattuso et al., 2019), and recently published literature as references, roughly 15 different expressions for K_1^* and K_2^* are currently in use, some of which are (partly) based on refitting data from earlier experiments (e.g. Dickson and Millero, 1987; Lueker et al., 2000); see Table S1 for an overview. Some expressions are based on measurements in artificial seawater of various compositions, while others were carried out in natural seawater. The vast majority of expressions were obtained in the laboratory under controlled conditions, using electrochemical cells either with (e.g. Millero et al, 2006; Millero, 2010) or without (e.g. Roy et al, 1993; Tishchenko et al., 2013) liquid junction. Within these cells, electromotive force readings of equilibrated seawater are used to compute equilibrium constants. Each expression is valid over its own range of T and S .

The various expressions for K_1^* and K_2^* obtained this way generally agree well, but discrepancies at low salinities have been highlighted (Cai and Wang, 1998; Millero, 2010; Dinauer and Mucci, 2017; Orr et al., 2018). In addition, the temperature range covered by various K_1^* and K_2^* expressions, although generally broad, only extends below 0 °C in a few studies (Millero et al., 2002; Goyet and Poisson, 1989; Papadimitriou et al, 2018). In fact, Mehrbach et al. (1973), who provided experimental data used by several authors to derive expressions for K_1^* and K_2^* (e.g., Dickson and Millero, 1987; Lueker et al., 2000), used data obtained at only four different temperatures (2, 13, 25 and 35 °C), which brings into question the accuracy of the temperature dependency of these constants. Bailey et al. (2018) recently suggested that the same bias exists for the dissolution of CO₂ in seawater and showed that previous expressions of Henry's Law constant for CO₂ underestimate the CO₂ solubility below 0 °C due to a lack of samples in cold waters. As explained by Raimondi et al. (2019), because the only carbonate system variables currently measured by in situ sensor technologies are pH and the partial pressure of CO₂ in seawater (pCO_2), relating laboratory or on-board measurements that are usually performed at temperatures ~25 °C to these in situ measurements requires an accurate knowledge of the K_1^* and K_2^* temperature dependency. About 40% of the ocean volume is at an average temperature lower than 2 °C, outside of the temperature range for which the Mehrbach et al. (1973) and derived constants are valid (from the data of Lauvset et al., 2016). An example of this are high-latitude cold waters, which are a critical component of the current global oceanic carbon cycle, as the Southern Ocean surface waters account for ~40% of the annual anthropogenic CO₂ uptake (Landschützer et al., 2015). Given past difficulties to obtain direct pCO_2 measurements from ships in the Southern Ocean (Bakker et al., 2016), a number of autonomous floats have been deployed in the recent years (see, e.g., Williams et al. (2017), Takeshita et al. (2018)). Since these floats estimate pCO_2 from a pH measurement and a calculated total alkalinity (TA), our knowledge of surface pCO_2 in the Southern Ocean strongly relies on the accuracy of dissociation constants in these cold waters.



95 Best practices for oceanic carbonate system measurements generally recommend the Lueker et al. (2000) constants
(Dickson et al., 2007), but the choice for a set of constants may depend on the environment and/or measured carbonate system
variables. Barring conditions where substantial impact of dissolved organic carbon on TA is expected (i.e. significant organic
alkalinity), only two of the measurable variables are required to characterize the whole carbonate system. Overdetermination
of the carbonate system, i.e., the concomitant measurement of at least three of the carbonate system variables (1) pCO_2 , (2)
100 DIC , (3) TA and (4) pH , is often used as a tool to identify the best pair of input variables for carbonate system calculations
under specific environmental conditions, e.g. in sea-ice brines (Brown et al., 2014) or in systems with substantial organic
alkalinity (Koeve and Oschlies, 2012). We refer the reader to Raimondi et al. (2019) for an overview of internal consistency
studies, i.e., the agreement between measured and calculated variables. Disagreement between measured and computed values
may arise from uncertainties in measurements and, more importantly, equilibrium constants (Orr et al., 2018), but can also
105 result from the choice of relationship between total boron and salinity, as well as organic alkalinity (Fong and Dickson, 2019).

Field measurements are rarely used to derive stoichiometric equilibrium constants because of their interdependence.
For example, ship-based measurements of pH are normally conducted at fixed temperature (commonly 25°C) and converted
to in situ temperature using a second input parameter as well as a set of stoichiometric equilibrium constants (Hunter, 1998).
110 Similarly, using measured TA to calculate the contribution of the carbonate system to total alkalinity (carbonate alkalinity, CA)
requires that the proton concentration and thus pH be known (Dickson et al., 2007). To the best of our knowledge, only two
studies have so far used overdeterminations of the carbonate system to derive expressions for K_1^* and K_2^* (Millero et al., 2002;
Papadimitriou et al, 2018). Both studies used concurrent measurements of pCO_2 , TA , DIC and pH over a range of temperatures
and salinities to calculate K_1^* and K_2^* . Millero et al. (2002) used over 6000 sets of pressure-corrected field measurements. They
115 argued that determinations of stoichiometric dissociation constants measured in natural seawater are preferable over those
determined in artificial seawater and concluded that the value of K_2^* depends on pCO_2 , possibly linked to organic alkalinity,
which is not accounted for in carbonate system calculations. Papadimitriou et al. (2018), who focussed especially on highly
saline brines down to their freezing points, used the same methods as Millero et al. (2002) for their calculations. However,
instead of using field measurements, they overdetermined their system under controlled laboratory temperatures and salinities,
120 thus avoiding temperature corrections of the pH measurements. Their work, like Orr et al. (2018), confirmed the high
uncertainties associated with extrapolating expressions for K_1^* and K_2^* beyond the investigated salinity and temperature ranges.

In the present study, we use the Global Ocean Data Analysis Project version 2 (GLODAPv2, Key et al., 2015; Olsen
et al., 2016) and the Surface Ocean CO₂ Atlas (SOCAT, Bakker et al., 2016) global data products to constrain stoichiometric
125 equilibrium constants based on surface-water field measurements. Using an iterative procedure that takes into account the lack
of independence of CA and pH , we quantify the temperature dependence of the stoichiometric equilibrium constants. We then
use these constants to recommend input pairs for pCO_2 and $CaCO_3$ saturation state determinations over various temperature
ranges and apply them onto a high-latitude data set.



2 Materials and Methods

130 2.1 Expressions for K_1^* and K_2^* as a function of carbonate system variables

Aside from recent advances that allow spectrophotometric determinations of CO_3^{2-} concentrations (Byrne and Yao, 2008; Easley et al, 2013; Sharp and Byrne, 2019), the concentrations of H_2CO_3^* , HCO_3^- and CO_3^{2-} are normally not directly measured in seawater. Instead, at least two of the four parameters $p\text{CO}_2$, $p\text{H}$, DIC and TA are measured, and the concentrations of the individual species inferred from them. In practical terms, TA is the sum of all bases that are titratable with a strong acid
135 to an equivalence point corresponding to the conversion of HCO_3^- to H_2CO_3^* . Here it is defined as:

$$\text{TA} = \text{CA} + \text{BA} + \text{PA} + \text{SiA} + [\text{OH}^-] - [\text{H}^+] \quad (6),$$

with $\text{CA} = [\text{HCO}_3^-] + 2[\text{CO}_3^{2-}]$, and where BA is the borate alkalinity ($[\text{B}(\text{OH})_4^-]$), PA is the phosphate alkalinity ($[\text{HPO}_4^{2-}] + 2[\text{PO}_4^{3-}] - [\text{H}_3\text{PO}_4]$), SiA is the silicate alkalinity ($[\text{SiO}(\text{OH})_3^-]$), $[\text{OH}^-]$ is the hydroxide ion concentration, and $[\text{H}^+]$ is the hydrogen ion concentration. Eq. (6) approximates the definition of TA provided by Dickson (1981), but does not take into account the hydrogen sulphide and ammonia acid-base systems. The terms BA , PA and SiA can all be expressed in terms of
140 stoichiometric equilibrium constants, total concentrations, and $[\text{H}^+]$. Hence, knowing TA , the total concentrations of dissolved silicate ($[\text{DSi}]$), soluble reactive phosphate ($[\text{SRP}]$) and boron, as well as $[\text{OH}^-]$ and $[\text{H}^+]$, CA can be calculated.

To estimate K_1^* and K_2^* as a function of salinity and temperature based solely on independent measurements, we first need to define expressions that define both constants as functions of CA , DIC , $p\text{CO}_2$ and $[\text{H}^+]$. Both K_1^* and K_2^* are normally
145 defined in terms of proton concentration, $[\text{H}^+]$, and the acid-base species they describe, see Eq. (4) and (5). In this work, we replace $[\text{H}_2\text{CO}_3^*]$, $[\text{HCO}_3^-]$ and $[\text{CO}_3^{2-}]$ by expressions that only contain the four variables present in the dataset and Henry's constant, K_0 , taken from Weiss (1974). This leads to the following set of equations, which are equivalent to those presented in Millero et al. (2002) and Papadimitriou et al. (2018):

$$K_1^* = \frac{[\text{H}^+](2\text{DIC} - \text{CA} - 2K_0p\text{CO}_2)}{K_0p\text{CO}_2} \quad (7),$$

$$150 \quad K_2^* = \frac{[\text{H}^+](\text{CA} - \text{DIC} + K_0p\text{CO}_2)}{2\text{DIC} - \text{CA} - 2K_0p\text{CO}_2} \quad (8).$$

Note that similar expressions can also be derived when only three independently measured variables are available in the dataset. In this case, either K_1^* or K_2^* remains in the expression, in addition to any three variables of the set CA , DIC , $p\text{CO}_2$ and $[\text{H}^+]$. Derivations of all these expressions can be found in the supplementary information.

155 2.2 Data

Data for T , P , practical salinity (S_p), DIC , TA , $p\text{H}$, $[\text{SRP}]$ and $[\text{DSi}]$ were taken from GLODAPv2 (Key et al., 2015; Olsen et al., 2016). Only data associated with a WOCE flag of 2, i.e., qualified as “acceptable”, were retained for this analysis.



Re-calculated or estimated variables and samples with missing T or S_p were always discarded. In total, we obtained 98326 samples for which TA , DIC and pH are available from independent, high-quality measurements.

160

pCO_2 values were obtained from SOCAT (Bakker et al., 2016). Only data associated with a WOCE flag of 2 are used. When available, a pCO_2 value was selected and added to corresponding surface GLODAPv2 samples. To select the most accurate pCO_2 value, we only merged GLODAPv2 and SOCAT samples from the same cruise and taken within the same hour; in most cases within the same 20 min. As a result, we assembled 1024 samples for which TA , DIC , pH and pCO_2 are all available from independent high-quality measurements. As underway pCO_2 measurements available in the SOCAT database are all from the surface ocean, it was not possible to assign measured pCO_2 values to samples at depth. Note that we discarded data from two cruises (EXPCODES #33AT20120419 and #49NZ20010828) for reasons explained in the supplementary information, ultimately using data from 948 samples for this analysis. Samples within this dataset were taken between 1993 and 2012 over 26 different research cruises. These samples were taken at the ocean surface, always in the top 5 meters. They cover a range of practical salinities from 30.73 to 37.57 and temperatures from -1.67 to 31.80 °C, at locations shown in Fig. 1.

170

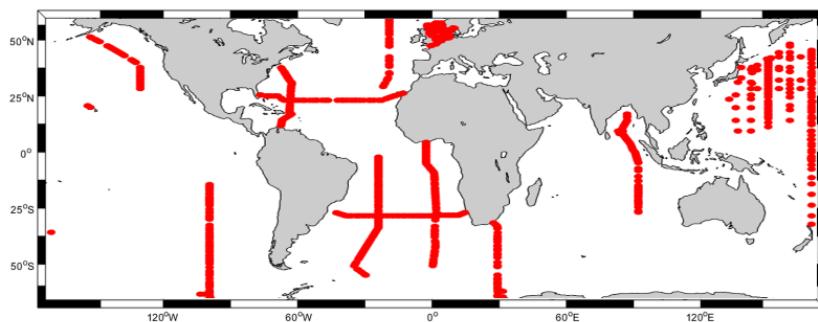


Figure 1. Spatial coverage of the dataset containing GLODAPv2 and SOCAT samples for which DIC , TA , pH and pCO_2 are available from independent, high-quality measurements.

175

2.3 Iterative methods and underlying assumptions

To the 948 samples for which independent, high-quality measurements of pH , DIC , TA , $[DSi]$, $[SRP]$ and pCO_2 are available, we would preferably directly apply Eq. (7) and (8). This was, however, not possible given the interdependence of pH and CA , both of which are necessary to compute K_1^* and K_2^* and, in turn, other carbonate system parameters. Rather than estimating the temperature dependence of pH from $\Delta pH/\Delta T$ as done by Millero et al. (2002), we used a novel iterative fitting procedure. This procedure is based on an initial estimate of both pH and CA using the Lueker et al. (2000) constants, followed by a re-computation at each iteration using the values of K_1^* and K_2^* from the previous iteration. The calculations were executed in R (R Core Team, 2019) and detailed below. The code and data files can be downloaded from an online repository (<https://doi.org/10.5281/zenodo.3725889>).

180



185

Since the objective of the present study is to obtain independent measurements of K_1^* and K_2^* , we could not directly use GLODAPv2 in situ pH data because the majority of these data were obtained on board by potentiometric or spectrophotometric methods at an equilibrium temperature often higher than the surface seawater (usually 25°C, occasionally 20 or 13°C). In addition, pH data were not always delivered to GLODAPv2 on the total pH scale. Consequently, the in situ pH measurements available in GLODAPv2 are all recalculated using measured TA and the Lueker et al. (2000) stoichiometric dissociation constants, and converted to the total pH scale if necessary (Olsen et al., 2016). To obtain the pH values delivered to GLODAPv2, which should be independent of K_1^* and K_2^* , we converted the GLODAPv2 pH values back to their measurement temperatures ($labT$) and pH scales, as recorded in the cruise reports. For this reversion, we used the bias-corrected TA value from GLODAPv2 rather than the measured TA values that were used in the GLODAPv2 conversion process. Bias correction of TA was done through crossover and inversion analysis of the data (Olsen et al., 2016); for the 26 research cruises we selected, bias correction resulted in TA adjustments of -1 to 10 $\mu\text{mol kg}^{-1}$. These adjustments however affected the recalculated pH values by less than 0.0001. We then converted all recalculated pH values to the free pH scale (pH_F^{labT}) using the default settings of the $pHconv$ function in the seacarb R package (Gattuso et al., 2019). The free pH scale was used during the fitting procedure to avoid further complications with the sulphate and fluoride acid-base systems. Nevertheless, final results are presented on the total pH scale.

Carbonate alkalinity was not directly measured, but is instead a pH -dependent quantity computed from TA , see Eq. (6). As a first approximation, we calculated CA from the measured TA by subtracting the contributions of the borate, silicate and phosphate acid-base systems, as well as the auto-dissociation of water, using $[SRP]$, $[DSi]$ and the in situ pH from GLODAPv2. We estimated the total boron concentration from salinity using the Uppström (1974) relationship and calculated its acid-base speciation using the equilibrium constants of Dickson (1990). For the silicate and phosphate acid-base speciation, the equilibrium constants of Yao and Millero (1995) were used. All of these expressions are only valid for temperatures above 0°C; thus, extrapolation to lower temperatures yields an additional uncertainty to the method. All equilibrium constants were corrected for pressure following Millero (1995), but given that all samples were taken at depth shallower than 5 m depth, this correction is negligible. Using H_F^{labT} , the proton concentration computed from pH_F^{labT} , we also calculated carbonate alkalinity at the temperature of pH measurements (CA^{labT}). This variable was used during the iteration procedure.

Since there are two pH -independent parameters (DIC , pCO_2), we can use these two parameters and one pH -dependent parameter (either pH itself, or CA) to initialise the iterative procedure. This implies that either K_1^* or K_2^* must be assigned an initial value before starting the iterations. Here, we initially set the in situ K_2^* to the value calculated from the Lueker et al. (2000) expressions. The alternative case in which in situ K_1^* was initially set to the Lueker et al. (2000) value is described in the supplementary information and would have no appreciable impact on the results presented here, i.e., whether the first or



the second dissociation constant is assigned an initial value does not affect the results. Each iteration consisted of four different steps:

220

(1) First, K_1^* was computed from in situ DIC , CA , pCO_2 and K_2^* from Lueker et al. (2000) using Eq. (7) and a Newton-Raphson technique (function *uniroot.all* from package *rootSolve*, Soetaert and Herman, 2009). These calculated K_1^* values were subsequently fitted to a general expression as a function of temperature and salinity of the form:

$$pK_{1 \text{ or } 2}^* = a_1 + a_2 S_P + a_3 S_P^2 + \frac{a_4}{T} + a_5 \ln(T) \quad (9),$$

225 where pK_i^* corresponds to $-\log_{10}(K_i)$ and a_i are fitting coefficients determined using the Levenberg-Marquardt algorithm for nonlinear least-squares estimates (function *nlsLM* from the *minpack.lm* package, Elzhov et al., 2016). This expression is of a similar form as Lueker et al. (2000), to facilitate the comparison. Because the salinity range in the sub-dataset where four carbonate system variables are available is narrow (30.73 to 37.57), it was not possible to obtain converging iterations where all the coefficients in Eq. (9) were resolved. Thus, we kept a_2 and a_3 fixed to the Lueker et al. (2000) values, assuming that the
 230 salinity dependence of K_1^* and K_2^* is correct for the salinity range of our dataset, and only solved for a_1 , a_4 and a_5 .

(2) Second, this new expression for K_1^* , as well as CA and the expression for K_2^* used in step 1, were used to compute pH at in situ temperature. For this, both K_1^* and K_2^* were calculated at the temperature of pH measurement ($K_1^{*,labT}$ and $K_2^{*,labT}$). These were used together with the free proton concentration at lab temperature (H_F^{labT}) and the calculated carbonate alkalinity
 235 (CA^{labT}), both of which do not change during the iterative procedure, to calculate $[H^+]$, the free proton concentration at in situ temperature. We expressed DIC as a function of CA , $[H^+]$, K_1^* and K_2^* , and assumed that the value of DIC is independent of temperature. Thus,

$$CA \frac{[H^+]^2 + [H^+]K_1^* + K_1^*K_2^*}{[H^+]K_1^* + 2K_1^*K_2^*} = CA^{labT} \frac{(H_F^{labT})^2 + H_F^{labT} K_1^{*,labT} + K_1^{*,labT} K_2^{*,labT}}{H_F^{labT} K_1^{*,labT} + 2K_1^{*,labT} K_2^{*,labT}} \quad (10)$$

This equation was rewritten into a quadratic equation, solved analytically for $[H^+]$, and converted to pH .

240

(3) Third, CA – which is dependent on pH – was updated based on the new $[H^+]$, as per Eq. (6) and the method outlined for the initial calculation of CA .

(4) Fourth, we used Eq. (8) to calculate K_2^* as a function of pCO_2 , DIC , the new pH and CA , and fit these in situ
 245 computed constants to an equation of the form of Eq. (9).

These four steps were repeated and at each iteration, K_2^* , CA , and pH from the previous iteration, were used as initial values. Note that this method assumes that the uncertainty in K_0 is minor compared to that in K_1^* and K_2^* . We also assumed that no acid-base systems other than the carbonate, borate, silicate and phosphate acid-base systems contributed to TA – this



250 point will be elucidated later – and that uncertainties in the calculated contributions of the latter three acid-base systems to TA were also minor compared to the uncertainties in K_1^* and K_2^* .

2.4 Uncertainty propagation

The overall uncertainty on the final K_1^* and K_2^* values is a combination of the uncertainties associated with measurement errors (hereafter termed “analytical uncertainty”) and the uncertainties resulting from the fitting procedures (hereafter termed “fitting uncertainty”), that are propagated throughout the iterations. The analytical uncertainty (σK^{ana}) was computed using the predefined accuracy limits (here, for simplicity, denoted σ) used for the GLODAPv2 secondary quality control procedures. This accuracy limit reflects the minimum bias that can be detected with reasonable certainty (Tanhua et al., 2010) and is based on an objective analysis of systematic biases in ship-based data. Within the GLODAP context the accuracy limit should be interpreted as “the range within which we can realistically expect measurements from the deep ocean to be reproducible”. For each variable the corresponding value is taken from Table 2 in Olsen et al. (2016), i.e., $\sigma S_p = 0.005$, $\sigma[DSi] = 2\%$, $\sigma[SRP] = 2\%$, $\sigma DIC = 4 \mu\text{mol kg}^{-1}$, $\sigma TA = 6 \mu\text{mol kg}^{-1}$. σpH is set to 0.01 following Table 3 in Olsen et al. (2019) and σpCO_2 is set to $2 \mu\text{atm}$, corresponding to the minimum accuracy of SOCAT quality control flags A or B. While referred to as accuracy this number is actually a measure of overall measurement uncertainty, and includes uncertainties due to environmental factors (Pierrot et al., 2009). σCA was computed as the square root of the sum of the squares of σCO_3^{2-} and σHCO_3^- . In turn, these were computed using TA , pH , $[SRP]$, $[DSi]$, P , T and S_p as input variables, as well as their respective aforementioned uncertainties, using the error propagation code of Orr et al. (2018). The analytical uncertainty on both K_1^* and K_2^* was then estimated following the standard rules of error propagation, as per the following equations:

$$\sigma K_1^{ana} = K_1^* \sqrt{\left(\frac{\sigma[H^+]}{[H^+]}\right)^2 + \left(\frac{\sigma fCO_2}{fCO_2}\right)^2 + \left(\frac{\sqrt{(2\sigma DIC)^2 + (\sigma CA)^2 + (2K_0 \sigma fCO_2)^2}}{2DIC - CA - 2K_0 fCO_2}\right)^2} \quad (11),$$

$$\sigma K_2^{ana} = K_2^* \sqrt{\left(\frac{\sigma[H^+]}{[H^+]}\right)^2 + \left(\frac{\sqrt{(\sigma CA)^2 + (\sigma DIC)^2 + (K_0 \sigma fCO_2)^2}}{CA - DIC + K_0 fCO_2}\right)^2 + \left(\frac{\sqrt{(2\sigma DIC)^2 + (\sigma CA)^2 + (2K_0 \sigma fCO_2)^2}}{2DIC - CA - 2K_0 fCO_2}\right)^2} \quad (12).$$

270

The fitting uncertainty (σK^{fit}) was obtained using a Monte Carlo simulation technique that propagates errors in the fitting coefficients to the predicted K values. At the end of the iterations, the non-linear least-square models fits obtained with the *nlsLM* function were used as an input in the *predictNLS* function, from the *propagate* R package (Spiess, 2018), to calculate σK^{fit} , neglecting any error in the temperature measurements. The overall uncertainty on K_1^* and K_2^* was then assumed to be the square root of the sum of the squares of the analytical and fitting uncertainties. The 95% confidence intervals for each of the fitting coefficients, i.e., a_i in Eq. (9), shown in Table 1, were extracted from the result of the non-linear least-squares model fit in R using the *summary* function. Note that, because we did not solve for the salinity coefficients in Eq. (10) due to the

275



limited salinity range of the four carbonate-system variables dataset, a_2 and a_3 are set to the Lueker et al. (2000) values and no confidence interval is computed for these coefficients.

280 3 Results

Table 1. Comparison of the coefficients for pK_1^* and pK_2^* between this study and Lueker et al. (2000), using an equation of the form of Eq. (9). Coefficients are given as value \pm 95% confidence interval.

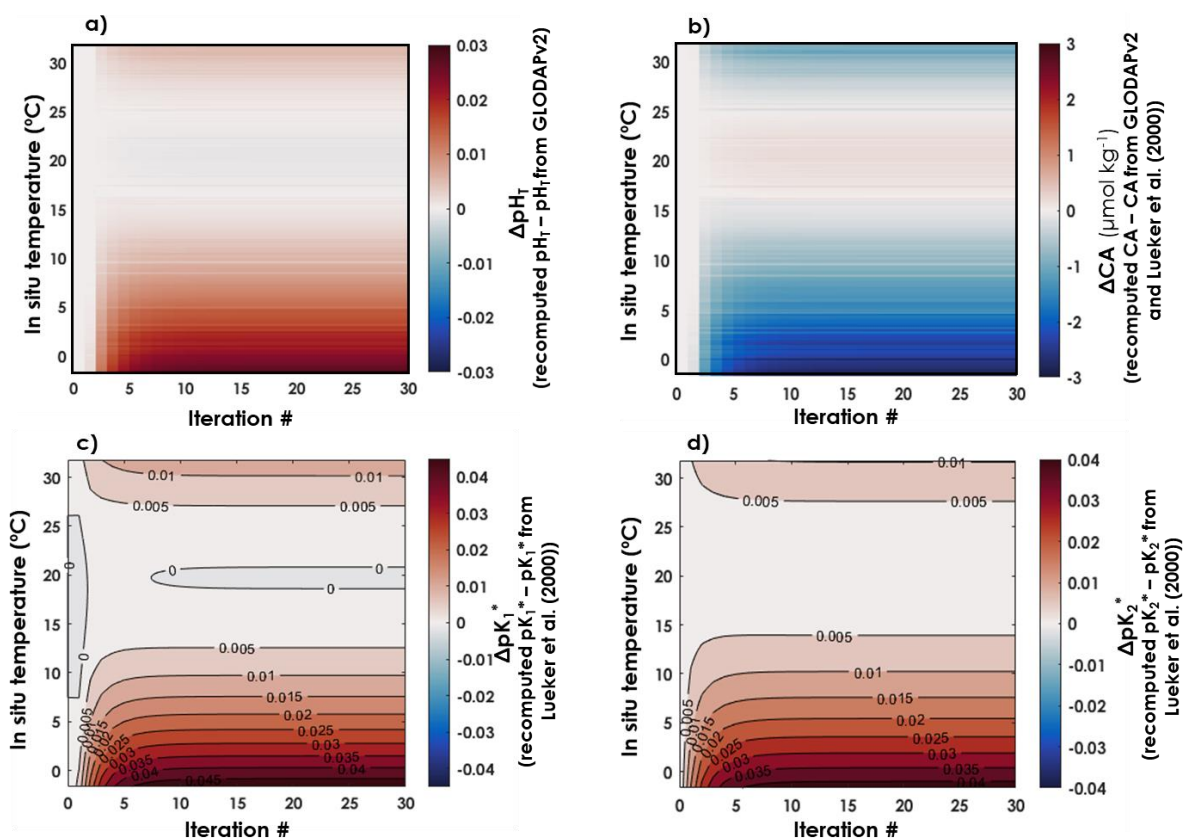
	This study		Lueker et al. (2000)	
	pK_1^*	pK_2^*	pK_1^*	pK_2^*
a_1	- 172.4493 \pm 26.131	- 59.4636 \pm 24.016	- 61.2172	25.9290
a_2	- 0.011555	- 0.01781	- 0.01155	- 0.017810
a_3	0.0001152	0.0001122	0.0001152	0.0001122
a_4	8510.63 \pm 1139.8	4226.23 \pm 1050.8	3633.86	471.78
a_5	26.32996 \pm 3.9161	9.60817 \pm 3.5966	9.67770	- 3.16967

As CA and pH are being updated throughout the iterations, CA , pH , K_1^* and K_2^* all evolved until the 10th iteration, before converging to a final value (Fig. 2). Thus, we stopped the iterative process after 30 iterations. Between the initial
 295 GLODAPv2 value and the 30th iteration, $[H^+]$ values vary by up to 6.6%. CA values are only weakly affected by these in situ pH updates as they change by a maximum of 0.2% throughout the first 30 iterations. Largest pH and CA changes occur in the colder end of the temperature range. pK_1^* and pK_2^* values both shift upward throughout the iterations, the pK_1^* increase being higher than that of pK_2^* , especially in cold waters (Fig. 2). Using all the data from which T , S_p , DIC , pH , CA and pCO_2 are available as high quality, independent measurements, we were able to derive expressions for K_1^* and K_2^* with a new
 300 temperature dependence. The coefficients a_i for pK_1^* and pK_2^* , in an equation of the form of Eq. (9), and after 30 iterations, are reported in Table 1, along with their respective 95% confidence intervals. In both expressions, all coefficients are significantly different from zero (p values $<$ 0.001).

As shown in Fig. 3, the pK^* values obtained with the iterative procedure are statistically indistinguishable from the
 305 pK^* values of Lueker et al. (2000) (i.e., $pK^{\text{this study}} - \sigma pK^{\text{this study}} < pK^{\text{Lueker}} < pK^{\text{this study}} + \sigma pK^{\text{this study}}$) over most of the temperature range. Nevertheless, in cold waters, below temperatures 8.1 and 9.2°C respectively, pK_1^* and pK_2^* are significantly higher than the values reported by Lueker et al. (2000). In Fig. 3, we also provide a comparison of the pK^* values of this study with those of Papadimitriou et al. (2018), as the latter study focuses on low-temperature waters. As shown in Figs. 3c,d, both pK_1^* and pK_2^* from Papadimitriou et al. (2018) are slightly lower than the fitted values from this study, for a similar salinity, and are



310 also lower than the Lueker et al. (2000) pK^* values except for temperatures below 4.0 and 1.2°C, respectively. Thus, that the Lueker et al. (2000) study underestimates both pK_1^* and pK_2^* in waters near freezing point seems to be a consistent feature across studies.



315

Figure 2. Evolution of pH_T , CA , pK_1^* and pK_2^* as a function of in situ temperature and iterations. a) Differences between recomputed pH_T and pH_T from GLODAPv2. b) Differences between recomputed CA and CA estimated from GLODAPv2 data and the Lueker et al. (2000) constants. Differences between recomputed c) pK_1^* and d) pK_2^* and the Lueker et al. (2000) values at in situ temperature and at a practical salinity of 35.

320

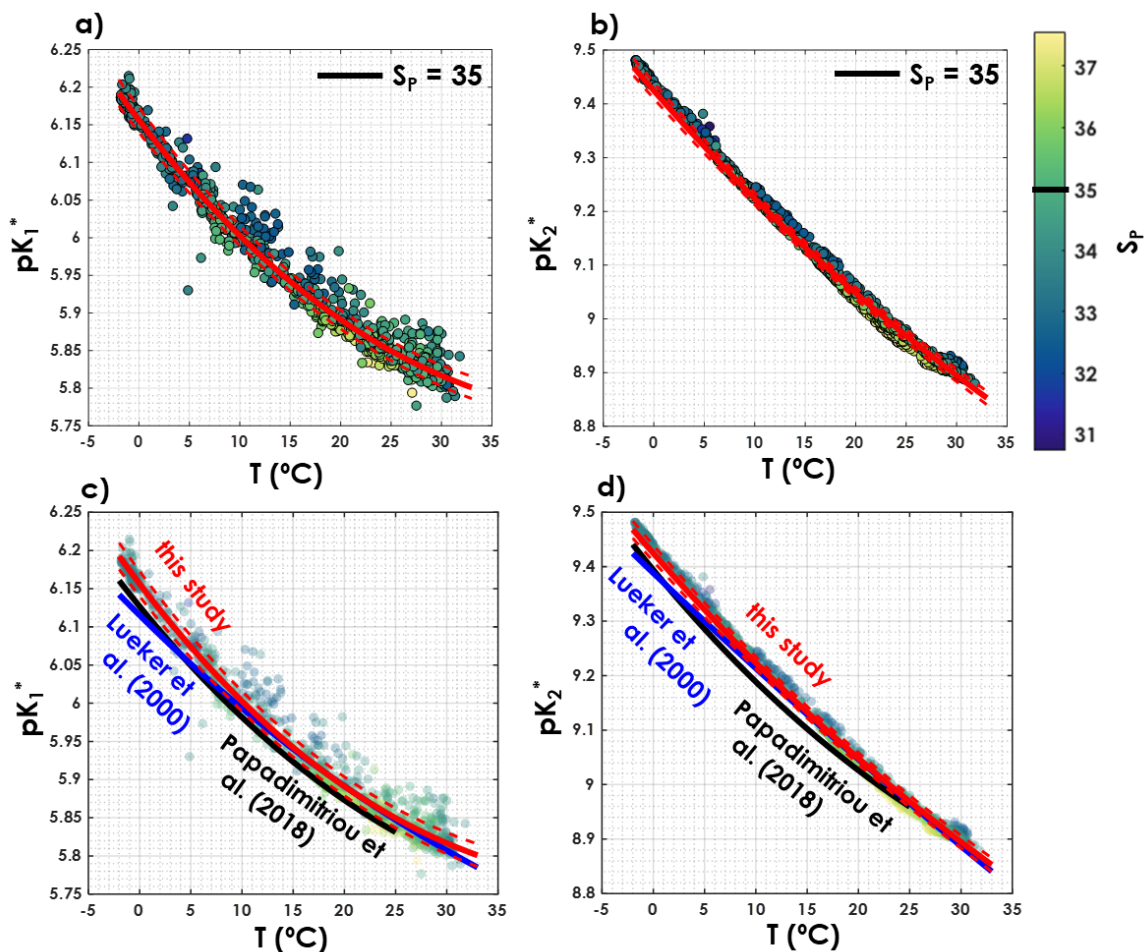


Figure 3. (a) pK_1^* and (b) pK_2^* as a function of temperature where the colour represents practical salinity (S_p), and the fits are fixed for a S_p of 35. Comparison of (c) pK_1^* and (d) pK_2^* as a function of temperature from this study (red lines), Lueker et al. (2000, blue line) and Papadimitriou et al. (2018, black line). The solid blue line represents the pK^* fits from Lueker et al. (2000), the solid red line the pK^* from this study computed with the coefficients presented in Table 1. Dashed red lines are overall uncertainties as defined in section 2.4.

325

330



4 Discussion

Using underestimated pK_1^* and pK_2^* values implies that, for a given state, computed $[\text{H}_2\text{CO}_3^*]$ or $p\text{CO}_2$ would be
335 underestimated and $[\text{CO}_3^{2-}]$ overestimated. This potentially has strong implications for our representation of seawater carbonate
chemistry in low-temperature marine environments, such as polar regions. Hence, we highlight the implications of this work
for the estimation of two carbonate system variables in polar regions, i.e. $p\text{CO}_2$ and the saturation state of seawater with respect
to calcite (Ω_{Ca}). But first, we examine error propagation and the dependence of pK_1^* and pK_2^* to salinity, and discuss the
influence of organic alkalinity and the quality of pH measurements on the results presented here.

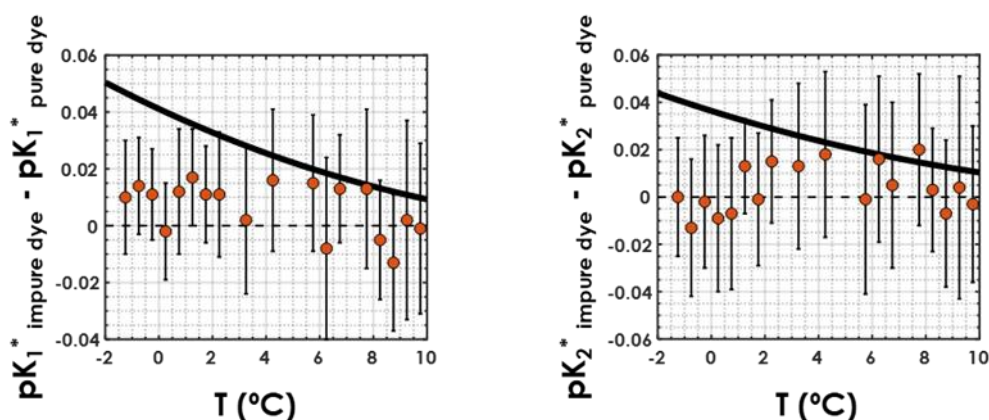
340 4.1 Influence of pH and TA measurement quality

The pH of samples that are used to derive the K^* fits presented here was measured using electrodes or
spectrophotometrically, between 1993 and 2012. During this period, it was shown that impurities present in commercially
available dyes could generate a systematic bias in the measured pH (Yao et al., 2007). Recently, Carter et al. (2018) pointed
out to the systematic discrepancies resulting from differing approaches to pH measurements. Yao et al. (2007) noted that these
345 impurities can contribute to pH offsets as large as 0.01 pH units, which corresponds to the analytical uncertainty in pH (σ_{pH})
that we use here, taken from Olsen et al. (2019). We must therefore investigate whether the fact that most pH measurements
in the pH dataset are not from spectrophotometric measurements with purified dyes could alter the conclusion of
underestimated pK^* values in cold waters. To answer this question, we gathered a sub-dataset of the more recent
GLODAPv2.2019 data product (Olsen et al., 2019), composed of samples from 9 different cruises (EXPCODES
350 #320620140320, #06AQ20150817, #33AT20120324, #33AT20120419, #33HQ20150809, #33RO20150410,
#33RO20150525, #33RO20161119 and #33RR20160208) for which T , P , S_p , DIC , TA , $[\text{SRP}]$ and $[\text{DSi}]$ are available and
associated with a WOCE flag of 2, for which pH was measured spectrophotometrically using purified dyes only, and for which
an associated SOCAT $p\text{CO}_2$ value is available. Although this independent dataset is too small to apply the iterative procedure
and obtain acceptable pK^* fits, we can use it to compare the K_1^* / K_2^* values obtained with Eqs. (7, 8) and this purified-dye
355 independent dataset to the K_1^* / K_2^* values obtained with Eqs. (7, 8) and the regular dataset.

For both the purified-dye independent dataset and the regular dataset, samples were sorted according to in situ
temperature and grouped into bins of 0.5 °C. Temperature bins containing a single sample were not used. For each temperature
bin, the mean pK^* values, obtained with Eqs. (7,8), along with the associated uncertainties, were computed. Plotting the
360 difference between the pK^* values computed using the regular dataset and those computed using the purified-dye independent
dataset as a function of seawater in situ temperature (Fig. 4), we do not see any clear systematic bias caused by the use of
purified dyes. This means that pK^* values computed from a dataset with purified-dye pH measurements only are not higher or
lower than pK^* values computed from a dataset with pH measured using primarily impure dye. More importantly, in colder
waters ($T < \sim 2$ °C), the differences between the pK^* values from this study and those from Lueker et al. (2000) (black line in



365 Fig. 4) are larger than what can be explained by the choice of dye for spectrophotometric pH measurements. Thus, the use of
impure vs. purified dye in pH measurements should not affect the conclusions presented here.



370 **Figure 4.** (left) pK_1^* and (right) pK_2^* differences between those obtained with the regular dataset and those
obtained with the purified-dye independent dataset, as a function of in situ seawater temperature. Orange circles
represent the mean computed pK^* values within a temperature bin, and the vertical black bars stand for the
associated uncertainties deviations. The solid black line is the difference between the pK^* fit from this study and
that from Lueker et al. (2000).

375

Another issue which GLODAPv2 carbonate system measurements may face is the fact that some seawater samples
contain measurable amounts of organic bases (Fong and Dickson, 2019; Patsavas et al., 2015; Yang et al., 2015). This organic
alkalinity is unaccounted for in the definition of total alkalinity of Eq. (6), thus causing biased, overestimated, computed
carbonate alkalinity values. This does not only concern coastal waters, but also open-ocean waters, where the total
concentration of these organic bases could be in the order of a few $\mu\text{mol kg}^{-1}$ (Fong and Dickson, 2019). This, however, should
not substantially alter the results presented here, due to the small amount of these organic bases and consequently small impact
on computed pK^* values. If any, subtracting the contributions of these unaccounted bases to the total alkalinity measurements
would have an unidirectional effect on the dissociation constant estimates, shifting the pK^* values upwards – see Eqs. (7,8) –
further away from the Lueker et al. (2000) values in cold waters.

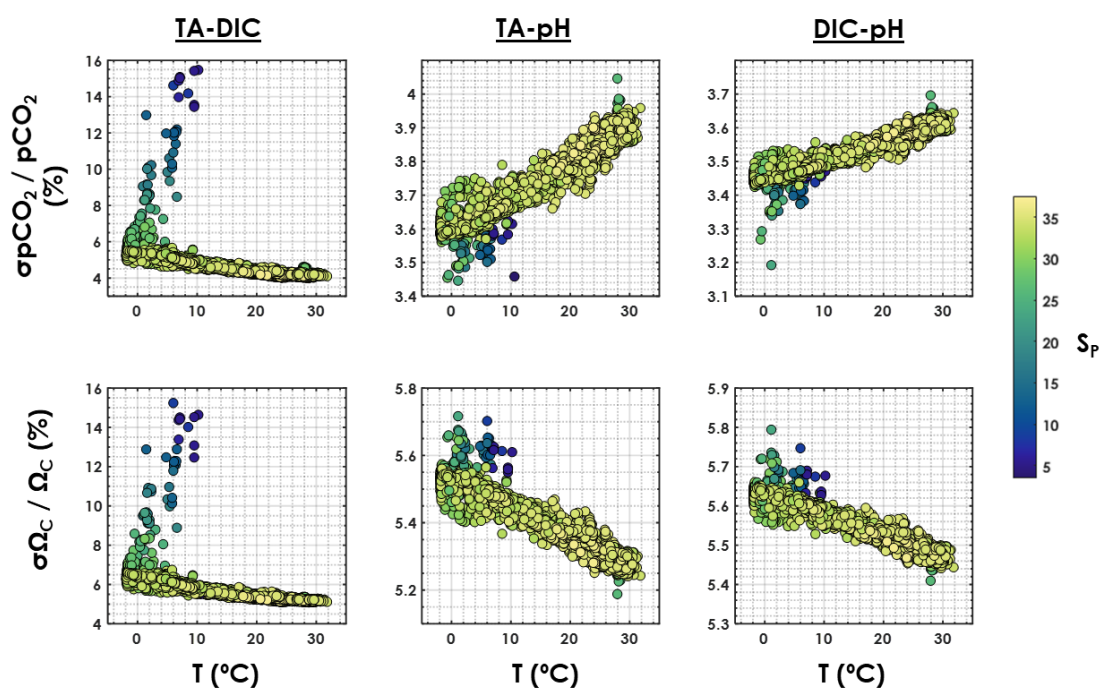
385

4.2 Uncertainties in carbonate system calculations

The relative overall uncertainties ($\sigma K^* / K^*$) were $\sim 2.5\%$ for both K_1^* and K_2^* . In both cases, the analytical uncertainty
(σK^{ana}) was more than twice as high as the fitting uncertainty (σK^{fit}). The overall pH measurement uncertainty of the GLODAP
dataset ($\sigma pH = 0.01$) is relatively high, causing the pH term in Eqs. (11,12) to be the dominant factor in σK^{ana} . Thus, what



390 dominates the overall uncertainties for K^* estimates from this study is the uncertainty in pH , which explains the fact that the
 relative uncertainties of K_1^* and K_2^* are similar. Converting from σK^* to σpK^* , we find $\sigma pK_1^* = \sigma pK_2^* = 0.011$. The overall
 uncertainty for pK_1^* is higher than that reported by Orr et al. (2018), but the overall uncertainty for pK_2^* is smaller. These
 values are quite high relative to the uncertainties of previous expressions for K_1^* and K_2^* as reported in Table 2 of Millero
 (2007), which we attribute to the fact that they reflect both the uncertainty from the fits and from the measurements that we
 395 use.



400 **Figure 5.** Overall relative uncertainty for (top) pCO_2 and (bottom) Ω_{Ca} as a function of in situ temperature
 (horizontal axis) and salinity (colour bar). The left column is for the TA-DIC pair, the central column is for the
 TA-pH pair and the right column is for the DIC-pH pair. This is computed using all data points from GLODAPv2
 that contain T , P , S_p , DIC , TA , pH , $[SRP]$ and $[DSi]$, in the top 10 meters of the water column (3392 samples).

Using the pK^* values from Table 1, setting the analytical uncertainties for each variable to the values reported in
 405 section 2.4, and using $\sigma pK_1^* = \sigma pK_2^* = 0.011$, we use the Excel version of CO2SYS from Orr et al. (2018) and analyse the
 propagation of uncertainties on two computed variables, pCO_2 and the saturation state of seawater with respect to calcite, Ω_{Ca}
 (Mucci et al., 1983, see discussion in section 4.3). For this purpose, we use all data points from GLODAPv2 that contain T , P ,
 S_p , DIC , TA , pH , $[SRP]$ and $[DSi]$, in the top 10 meters of the water column. The quality criteria remains unchanged, i.e., we
 use only data associated with a WOCE flag of 2, i.e., qualified as “acceptable”. The obtained dataset contains 3392 samples,

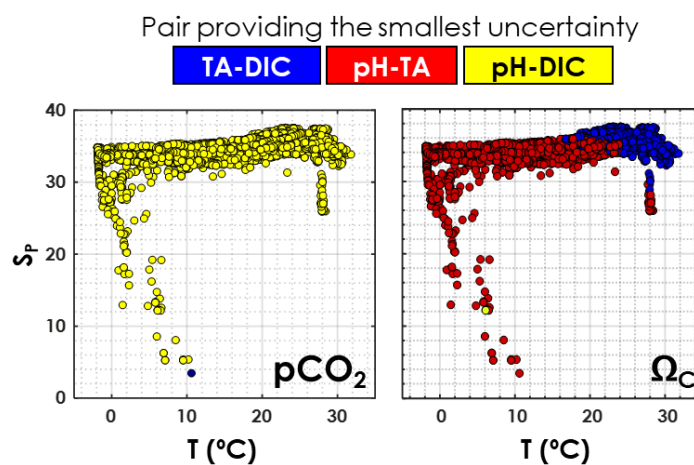


410 including the 948 samples of the regular dataset, covers a salinity range from 3.46 to 37.57 and a temperature range from -1.91
to 31.80 °C. Depending on which carbonate-system pair of variables is used, both the magnitude and the uncertainties of
computed variables can differ (Orr et al., 2018; Ribas-Ribas et al., 2014). Here, we use three different pairs of variables, i.e.
TA-DIC, *TA-pH* and *DIC-pH*, to compute pCO_2 and Ω_{Ca} and their associated propagated uncertainties, σpCO_2 and $\sigma\Omega_{Ca}$,
respectively.

415

Relative uncertainties generated with the *TA-DIC* pair appear to be particularly sensitive to salinity (Fig. 5), increasing
from ~5 to ~15% for both pCO_2 and Ω_{Ca} as the salinity decreases from 35 to 5. The overall relative uncertainty for both pCO_2
and Ω_{Ca} is less dependent on salinity when pH is used as an input variable with either *DIC* or *TA*. For both the *TA-pH* and the
DIC-pH pairs, the overall relative uncertainty on pCO_2 increases with an increasing temperature, while the overall relative
420 uncertainty on Ω_{Ca} decreases with an increasing temperature (Fig. 5).

As depicted in Fig. 6, in agreement with Raimondi et al. (2019), we conclude that the *DIC-pH* pair offers the lowest
overall relative uncertainty for computed pCO_2 over the range of salinities and temperatures investigated. Using the *DIC-pH*
pair also has the important benefit of not having to make any assumption regarding organic alkalinity or the boron to salinity
425 ratio (Fong and Dickson, 2019). Conversely, the *TA-pH* pair is the one generating the highest overall relative uncertainties on
computed pCO_2 . As for Ω_{Ca} , the *TA-pH* pair provides the lowest overall relative uncertainty below a temperature of ~20 °C,
whereas the *TA-DIC* pair should be preferred in warmer waters (Fig. 6).



430 **Figure 6.** Pair of carbonate system variables (*TA-DIC*, *TA-pH* or *DIC-pH*) providing the lowest overall relative
uncertainty, as a function of in situ temperature and practical salinity, for pCO_2 and Ω_{Ca} . This is computed using
all data points from GLODAPv2 that contain T , P , S_p , DIC , TA , pH , $[SRP]$ and $[DSi]$ in the top 10 meters of the
water column (3392 samples).



435 4.3 Implications for surface ocean $p\text{CO}_2$

To evaluate the implications of the revised temperature dependence of the carbonic acid dissociation constants, we compare ocean carbonate chemistry as calculated with the constants from this study, those of Lueker et al. (2000) and those of Millero et al. (2002). Whereas the constants from Lueker et al. (2000) are the most commonly used by the oceanographic community, as recommended by Dickson et al. (2007), the constants from Millero et al. (2002) were derived in an approach similar to that presented here, using a large dataset of in situ measurements. Thus, it appears relevant to include a comparison with Millero et al. (2002) in the present discussion. The major differences between our approach and the approach of Millero et al. (2002) are the calculation of CA from measured TA and pH (iteratively versus direct) and the conversion of pH measurements (iteratively versus estimating $\Delta pH/\Delta T$ from the constants of Mehrbach et al. (1973)).

445 For this comparison, we use data from the Southern Ocean Carbon and Climate Observations and Modelling (SOCCOM) project (<https://socom.princeton.edu/>). The SOCCOM project has deployed more than 100 Argo floats equipped with biogeochemical sensors in the Southern Ocean. These sensors include pH , and SOCCOM routinely calculate the full carbon chemistry (including $p\text{CO}_2$ and Ω_{Ca}) using a combination of measured T , S_P , pH , O_2 , and empirical algorithms for TA (Carter et al., 2018). The SOCCOM data used here, both measured and calculated, were downloaded as a Matlab file from
450 <https://library.ucsd.edu/dc/object/bb0515927k>.

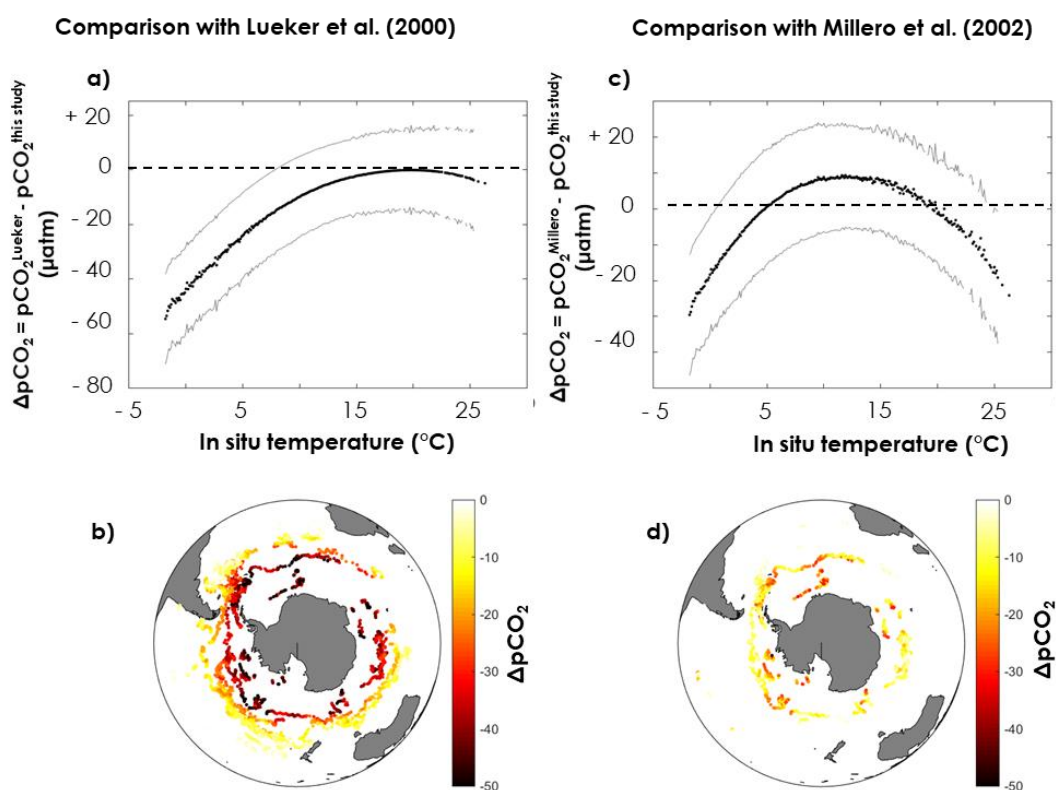
The method used to calculate $p\text{CO}_2$ is detailed in the data file (within the *FloatViz* structure). Briefly, they use the Lueker et al. (2000) K_1^* and K_2^* , Perez and Fraga (1987) for K_F , Dickson (1990) for K_{SO_4} , and Lee (2010) for total boron estimates. Both $[DSi]$ and $[SRP]$ are estimated from the measured nitrate concentration using stoichiometric ratios of 2.5 and
455 1/16, respectively. We applied the same method but substituted the Lueker et al. (2000) K_1^* and K_2^* constants with either the constants from this study or the Millero et al. (2002) constants. We were then able to compare surface-ocean (defined as the upper 10 m of the water column) $p\text{CO}_2$ obtained using Lueker et al. (2000) or Millero et al. (2002) with $p\text{CO}_2$ obtained using the constants from this study. The analytical uncertainties were set to $\sigma_{S_P} = 0.005$ and $\sigma_T = 0.005$ °C (Olsen et al., 2016), $\sigma[DSi] = 0.9$ $\mu\text{mol kg}^{-1}$ and $\sigma[SRP] = 0.5$ $\mu\text{mol kg}^{-1}$ (combination of uncertainty in nitrate concentration from Argo data, i.e.,
460 0.5 $\mu\text{mol kg}^{-1}$ as given in Johnson et al. (2017) and a 30% uncertainty in stoichiometric ratios), $\sigma_{TA} = 5.6$ $\mu\text{mol kg}^{-1}$ (Carter et al., 2018) and $\sigma_{pH} = 0.005$ (Johnson et al., 2017). $\sigma_{pK_1^*}$ and $\sigma_{pK_2^*}$ were set to 0.011, respectively, when the constants from this study were used. For both Lueker et al. (2000) or Millero et al. (2002), they were set to the default values given by Orr et al. (2018), i.e., $\sigma_{pK_1^*} = 0.0075$ and $\sigma_{pK_2^*} = 0.015$. Uncertainties on the computed $p\text{CO}_2$ were propagated using the Matlab version of the Orr et al. (2018) CO2SYS software with error propagation.

465

$p\text{CO}_2$ values obtained with the constants derived from this study are clearly higher than the Lueker et al. (2000)-based values in the southernmost regions, where temperatures are lowest (Fig. 7a,b), with a maximum difference ($\Delta p\text{CO}_2 = p\text{CO}_2^{\text{Lueker}}$



470 $-pCO_2^{\text{this study}}$) of $-55 \pm 17 \mu\text{atm}$ when the surface ocean is near the freezing point. The uncertainty on ΔpCO_2 ($\sigma\Delta pCO_2$, gray lines in Fig. 7) is computed as the square root of the sum of the squares of $\sigma pCO_2^{\text{Lueker}}$ and $\sigma pCO_2^{\text{this study}}$. Given the large uncertainties, the pCO_2 difference between values based on constants derived from this study and values based on Lueker et al. (2000) is only statistically significant (i.e., $\Delta pCO_2 + \sigma\Delta pCO_2^{\text{this study}} < 0$) for temperatures below $\sim 8^\circ\text{C}$ (Fig. 7a). pCO_2 values obtained using Millero et al. (2002) constants appear to be midway between pCO_2 values obtained using Lueker et al. (2000) constants, and pCO_2 values based on the constants from this study (Fig. 7c,d).



475

480

Figure 7. Difference in surface pCO_2 obtained from pH, temperature, practical salinity and dissolved oxygen measured by the SOCCOM Argo array using (left) the Lueker et al. (2000) constants and the constants in Table 1, or (right) the Millero et al. (2002) constants and the constants in Table 1. Plots (a,c) represents the pCO_2 difference (ΔpCO_2) as a function of in situ temperature. Solid black lines are the mean ΔpCO_2 while solid gray lines are plus or minus $\sigma\Delta pCO_2$ (square root of the sum of the squares of $\sigma pCO_2^{\text{Lueker}}$ and $\sigma pCO_2^{\text{this study}}$). Maps (b,d) depict the spatial distribution of ΔpCO_2 in the Southern Ocean, where each point corresponds to an Argo float measurement.



485 Recently the SOCCOM Argo array was used to re-evaluate the Southern Ocean carbon sink (Gray et al., 2018).
Traditional ship-based observations indicate a strong CO₂ uptake in the entire Southern Ocean, but these observations are
known to have a strong seasonal bias (Bakker et al. 2016), as well as a smaller spatial bias due to many areas being severely
undersampled (Takahashi et al., 2012). Using pCO_2 calculated by the above method, Gray et al. (2018) showed that the
Southern Ocean CO₂ uptake is considerably smaller than previously estimated. Since the Southern Ocean is one of the strongest
490 regional ocean carbon sinks this has severe impacts for our understanding of the global ocean carbon sink. Bailey et al. (2018)
showed that the CO₂ solubility constant from Weiss et al. (1974) used in the majority of studies, including this one, was
underestimated in waters below 0 °C, which implies that surface pCO_2 is underestimated. Using the new constants in Table 1,
Southern Ocean pCO_2 is significantly higher than the values used by Gray et al. (2018), meaning that the air-sea CO₂ fluxes
are much smaller, in agreement with the conclusions of Bailey et al. (2018). The ocean CO₂ sink is immensely important, and
495 currently estimated to remove ~25% of anthropogenic CO₂ emissions (Le Quéré et al., 2018). If the CO₂ uptake by the Southern
Ocean is much smaller than previously estimated, there must be missing sinks elsewhere in the Earth System, be it in the
oceanic or terrestrial realm. This highlights the need for a better understanding of the dynamics of the ocean carbon sink,
including its regional and temporal variability. To validate our results, the high uncertainties associated with stoichiometric
constants (Orr et al., 2018), coupled to the low spatial and temporal resolution of measurements in high latitudes, need to be
500 addressed. Whether in the laboratory or in the field, future work should focus on a better understanding of seawater carbonate
chemistry in cold waters.

4.4 Implications for calcium carbonate chemistry

In seawater undersaturated with respect to calcite or aragonite, (Ω_{Ca} or $\Omega_{Ar} < 1$), the CaCO₃ phase of interest should
505 dissolve if present. Ω_{Ca} depends on the Ca²⁺ concentration in seawater (a function of salinity and therefore nearly invariant at
depth), the solubility product of calcite (Mucci, 1983) and the CO₃²⁻ concentration in seawater. Because of the latter, computed
 Ω_{Ca} values are impacted by the choice of carbonic acid dissociation constants. Note that, as reported in Orr et al. (2018), the
relative uncertainty on the solubility product of calcite is about 5%. Below, we test the implications of the K_1^* and K_2^* values
from this study on predictions of calcite saturation state in seawater.

510

Naviaux et al. (2019) recently observed discrepancies between Ω_{Ca} computed with the $TA-DIC$ pair and Ω_{Ca} computed
with the $TA-pH$ pair, that they attributed to the internal inconsistency of the carbonate system, i.e., the fact that measured pH
does not correspond to calculated pH . Instead, or in addition, the calcite saturation depth calculated by Naviaux et al. (2019)
could be erroneously too shallow due to an overestimated K_2^* and, consequently, overestimated seawater [CO₃²⁻] and Ω_{Ca} .

515

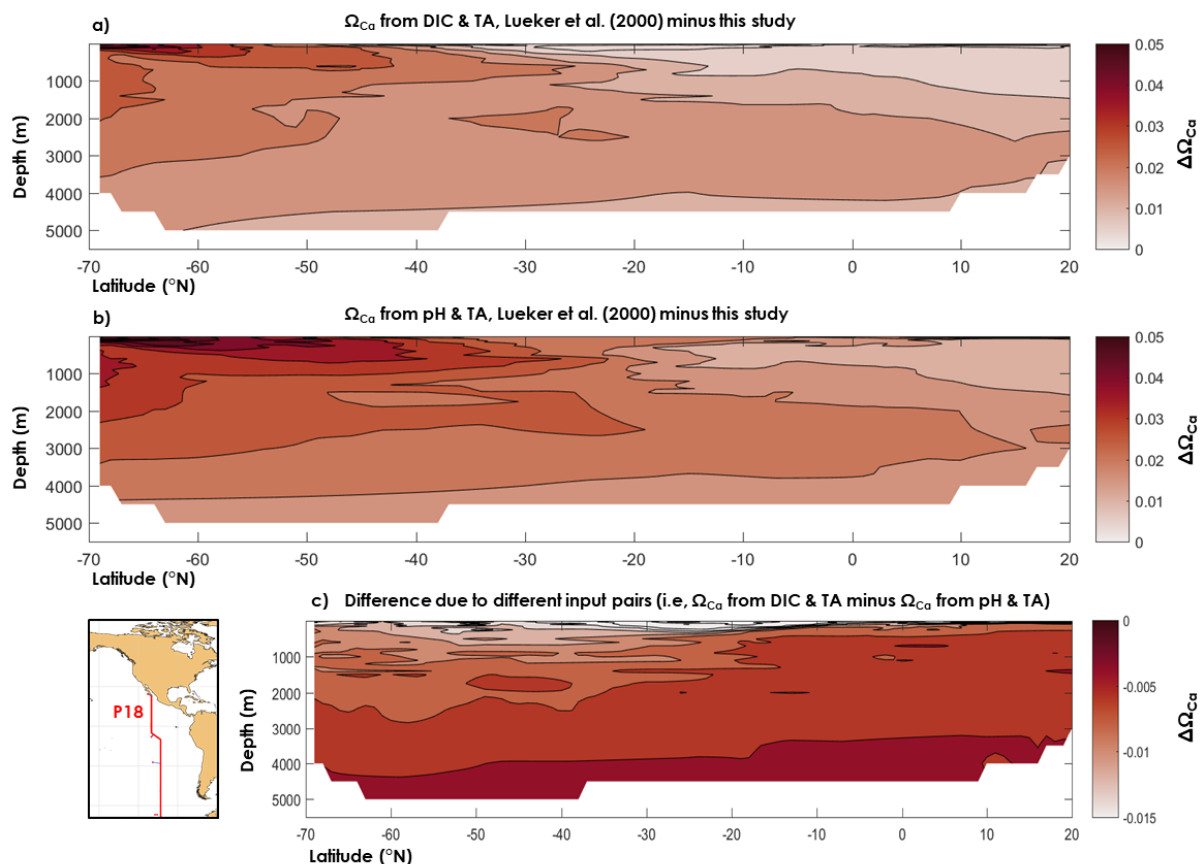


Figure 8. Difference between a) the calcite saturation state (Ω_{Ca}) computed from TA and DIC using the dissociation constants of Lueker et al. (2000) and the constants derived from this study, b) Ω_{Ca} computed from pH and TA using the dissociation constants of Lueker et al. (2000) and the constants derived from this study and c) Ω_{Ca} computed from the DIC and TA pair and the pH and TA pair, and the dissociation constants derived from this study.

Here, we used data from a cruise (#33RO20071215, GLODAPv2 cruise #345) along the CLIVAR repeat section P18 that took place in 2007, following a latitudinal transect in the south-eastern Pacific Ocean, in which the carbonate chemistry variables *DIC*, *TA* and *pH* were measured (see Olsen et al. (2016) for details about the data). All calculations were carried out using the discrete data, but for purposes of visualisation (Fig. 8) we used a nearest neighbour interpolation (function *griddata* in Matlab). In Fig. 8, we compare Ω_{Ca} as computed using K_1^* and K_2^* from this study, with Ω_{Ca} based on Lueker et al. (2000) constants. We also compare Ω_{Ca} computed from *TA-DIC* with Ω_{Ca} computed from *TA-pH*. From Fig. 8, it can be seen that the Ω_{Ca} difference between two different carbonate system pairs (*TA-DIC*, *TA-pH*) is ~ 5 times smaller than the Ω_{Ca} difference that is due to the set of dissociation constants. Thus, the apparent dissolution observed by Naviaux et al. (2019) may be



explained by overestimated dissociation constants atop inconsistencies arising from the choice of carbonate variables used in the calculations. We also note, based on Fig. 8, that Ω_{Ca} overestimation is largest in the southernmost part of the Pacific surface waters, where the temperature is the lowest. Nevertheless, the maximum calculated Ω_{Ca} differences, i.e., $\Delta\Omega_{Ca} = 0.06$ with $TA-$
535 DIC and $\Delta\Omega_{Ca} = 0.07$ with $TA-pH$, is 2-3 times lower than the average combined uncertainty, i.e., $((\sigma\Omega_{Ca}^{Lueker})^2 + (\sigma\Omega_{Ca}^{this\ study})^2)^{0.5} = 0.20$ and 0.17 , respectively. These high uncertainties are attributed to the high measurement uncertainties that we use (those from Olsen et al., 2016, see section 2.4), the overall uncertainty on the dissociation constants from this study, the uncertainty on Lueker et al. (2000) constants, but especially to the uncertainty in the calcite solubility product. As noted by
540 Orr et al. (2018), the uncertainty on the calcite solubility product (~5%) causes the total uncertainty on Ω_{Ca} to be considerably larger than the uncertainty in seawater $[CO_3^{2-}]$. In this study, only the K_1^* and K_2^* constants have been re-evaluated, but the large overall uncertainties on calculated saturation states clearly indicate that more work is necessary to define the solubility products of calcium carbonate minerals in the ocean. While beyond the scope of the present study, the results presented here show that proper assessments of present and future ocean acidification are highly sensitive to the present knowledge gaps regarding the thermodynamics of ocean carbon chemistry.

545

5 Conclusion

An iterative procedure allowed us to estimate the temperature dependence of the first and second carbonic acid stoichiometric dissociation constants (K_1^* and K_2^* , respectively) from a large dataset of high-quality oceanographic measurements. Both K_1^* and K_2^* were similar to the constants of Lueker et al. (2000) that are currently used by most of the
550 oceanographic community, as recommended by Dickson (2007), but the K_1^* and K_2^* values were lower in cold seawater, below a temperature of ~8-9 °C. Consequently, at these temperatures, pCO_2 computed using the constants of Lueker et al. (2000) may be underestimated and $[CO_3^{2-}]$ overestimated, meaning that the cold oceans are more undersaturated with respect to $CaCO_3$ minerals than expected. We also used a GLODAP sub-dataset to study the internal consistency of the carbonate system and found that the $DIC-pH$ carbonate system pair provides the smallest overall uncertainty when computing seawater
555 pCO_2 . When calculating the saturation state of seawater with respect to calcite, the $TA-DIC$ pair should be used to minimize the overall uncertainty when seawater is warmer than ~20 °C, whereas the $TA-pH$ pair should be preferred below ~20 °C. These results are of critical importance for scientists contemplating studies of high-latitude marine carbonate chemistry and underline that improved knowledge of what causes the CO_2 system inconsistencies in cold waters is key to improve our understanding of the marine carbon budget.



560

Data availability

The R code and data files are available on Zenodo (<https://doi.org/10.5281/zenodo.3725889>).

Author contribution

OS conceived the original idea, OS and MH designed the research, MH wrote the code and SKL advised on the use of the
565 GLODAPv2, SOCAT and Argo datasets.

Competing interests

The authors declare that they have no conflict of interest.

Acknowledgements

We thank Dorothee C. E. Bakker and Mariana Ribas Ribas for fruitful discussions, Alfonso Mucci and Andrew Dickson for
570 helpful comments and suggestions on an earlier version of the manuscript. We thank all who contributed to the creation of
GLODAPv2 and SOCAT. OS acknowledges the Department of Earth and Planetary Sciences at McGill University for financial
support during his residency in the graduate program and acknowledges funding from the Dutch Ministry of Education via the
Netherlands Earth System Science Centre (NESSC). SKL acknowledges funding from the Research Council of Norway
through (ICOS-Norway, 245927).

575 References

- Aman, A. A. and Bman, B. B.: The test article, *J. Sci. Res.*, 12, 135–147, doi:10.1234/56789, 2015.
- Aman, A. A., Cman, C., and Bman, B. B.: More test articles, *J. Adv. Res.*, 35, 13–28, doi:10.2345/67890, 2014.
- Archer, D., Eby, M., Brovkin, V., Ridgwell, A., Cao, L., Mikolajewicz, U., Caldeira, K., Matsumoto, K., Munhoven, G.,
Montenegro, A., Tokos, K. 2009. Atmospheric Lifetime of Fossil Fuel Carbon Dioxide. *Annual Rev. Earth Pl. Sc.* 37, 117-
580 134, <https://doi.org/10.1146/annurev.earth.031208.100206>
- Anes, B., Bettencourt da Silva, R.J.N., Oliveira, C., Camões, M.F., 2018. Uncertainty evaluation of alkalinity measurements
on seawater samples. *Measurement* 129, 395-404.
- Bakker, D.C.E., Pfeil, B., Landa, C.S., Metzl, N., O'Brien, K.M., Olsen, A., ... Nakaoka, S.I., Smith, K., Cosca, C., Harasawa,
S., Jones, S.D., Nakaoka, S.-i., Nojiri, Y., Schuster, U., Steinhoff, T., Sweeney, C., Takahashi, T., Tilbrook, B., Wada, C.,
585 Wanninkhof, R., Alin, S.R., Balestrini, C.F., Barbero, L., Bates, N.R., Bianchi, A.A., Bonou, F., Boutin, J., Bozec, Y., Burger,
E.F., Cai, W.-J., Castle, R.D., Chen, L., Chierici, M., Currie, K., Evans, W., Featherstone, C., Feely, R.A., Fransson, A., Goyet,
C., Greenwood, N., Gregor, L., Hankin, S., Hardman-Mountford, N.J., Harlay, J., Hauck, J., Hoppema, M., Humphreys, M.P.,



- Hunt, C.W., Huss, B., Ibáñez, J.S.P., Johannessen, T., Keeling, R., Kitidis, V., Körtzinger, A., Kozyr, A., Krasakopoulou, E., Kuwata, A., Landschützer, P., Lauvset, S.K., Lefèvre, N., Lo Monaco, C., Manke, A., Mathis, J.T., Merlivat, L., Millero, F.J., Monteiro, P.M.S., Munro, D.R., Murata, A., Newberger, T., Omar, A.M., Ono, T., Paterson, K., Pearce, D., Pierrot, D., Robbins, L.L., Saito, S., Salisbury, L., Schlitzer, R., Schneider, B., Schweitzer, R., Sieger, R., Skjelvan, I., Sullivan, K.F., Sutherland, S.C., Sutton, A.J., Tadokoro, K., Telszewski, M., Tuma, M., van Heuven, S.M.A.C., Vandemark, D., Ward, B., Watson, A.J., Xu, S. 2016. A multi-decade record of high-quality fCO₂ data in version 3 of the Surface Ocean CO₂ Atlas (SOCAT), *Earth Syst. Sci. Data* 8(2), 383–413.
- 590
- Bates, N.R. 2019. Ocean Carbon Cycle. In: Cochran, J.K., Bokuniewicz, H.J., Yager, P.L. (Eds), *Encyclopedia of Ocean Sciences (Third Edition)*. Elsevier. Vol. 1, pp. 418-428.
- 595
- Bailey, N., Papakyriakou, T.N., Bartels, C., Feiyue, W. 2018. Henry's Law constant for CO₂ in aqueous sodium chloride solutions at 1 atm and sub-zero (Celsius) temperatures. *Mar. Chem.* 207, 26-32. <https://doi.org/10.1016/j.marchem.2018.10.003>
- 600
- Berelson, W.M., Balch, W.M., Najjar, R., Feely, R.A., Sabine, C., Lee, K. 2007. Relating estimates of CaCO₃ production, export, and dissolution in the water column to measurements of CaCO₃ rain into sediment traps and dissolution on the sea floor: A revised global carbonate budget. *Global Biogeochem. Cy.* 21(1), <https://doi.org/10.1029/2006GB002803>
- Berner, R.A., Mackenzie, F.T. 2011. Burial and Preservation of Carbonate Rocks Over Phanerozoic Time. *Aquat. Geochem.* 17, 727-733.
- 605
- Betzer, P.R., Byrne, R.H., Acker, J.G., Lewis, C.S., Jolley, R.R., Feely, R.A. 1984. The oceanic carbonate system: a reassessment of biogenic controls. *Science* 226(4678), 1074-1077.
- Bishop, J.K.B., Stepien, J.C., Wiebe, P.H. 1986. Particulate matter distributions, chemistry and flux in the panama basin: response to environment forcing. *Prog. Oceanogr.* 17, 1-59.
- Brown, K.A., Miller, L.A., Davelaar, M., Francois, R., Tortell, P.D. 2014. Over-determination of the carbonate system in natural sea-ice brine and assessment of carbonic acid dissociation constants under low temperature, high salinity conditions. *Mar. Chem.* 165, 36-45. <https://doi.org/10.1016/j.marchem.2014.07.005>
- 610
- Buch, K. 1930. Die Kohlensäurefaktoren des Meerwassers. *Rapp. P.-V. Réun Cons. Perm. Int. Explor. Mer*, 67, 51-88.
- Buch, K. 1938. New determinations of the second dissociation constant of carbonic acid in sea water. *Acta Acad. Abo. (Math. Phys.)*, 11(5), 18 pp.
- 615
- Byrne, R.H., Acker, J.G., Betzer, P.R., Feely, R.A., Cates, M.H. 1984. Water column dissolution of aragonite in the Pacific Ocean. *Nature* 312, 321-326.
- Byrne, R.H., Yao, W., 2008. Procedures for measurement of carbonate ion concentrations in seawater by direct spectrophotometric observations of Pb(II) complexation. *Mar. Chem.* 112 (1), 128–135.
- Cai, W.-J., Wang, Y. 1998. The chemistry, fluxes, and sources of carbon dioxide in the estuarine waters of the Satilla and Altamaha Rivers, Georgia. *Limnol. Oceanogr.* 43(4), 657-668.
- 620
- Carter, B.R., Feely, R.A., Williams, N.L., Dickson, A.G., Fong, M.B., Takeshita, Y. 2018. Updated methods for global locally interpolated estimation of alkalinity, pH, and nitrate. *Limnol. Oceanogr.-Meth.* 16 (2), 119-131.
- Chierici, M., Fransson, A. 2009. Calcium carbonate saturation in the surface water of the Arctic Ocean: undersaturation in freshwater influenced shelves. *Biogeosciences* 6, 2421-2432.
- 625
- Dickson, A.G. 1981. An exact definition of total alkalinity and a procedure for the estimation of alkalinity and total inorganic carbon from titration data. *Deep-Sea Res.* 28A(6), 609-623.
- Dickson, A.G. 1990. Thermodynamics of the dissociation of boric acid in synthetic seawater from 273.15 to 318.15 K. *Deep-Sea Res.* 37(5), 755-766.



- 630 Dickson, A.G., Millero, F.J. 1987. A comparison of the equilibrium constants for the dissociation of carbonic acid in seawater media. *Deep-Sea Res.* 34(10), 1733-1743.
- Dickson, A.G.; Sabine, C.L., Christian, J.R. 2007. Guide to best practices for ocean CO₂ measurement. Sidney, British Columbia, North Pacific Marine Science Organization, 191pp. PICES Special Publication 3. <http://hdl.handle.net/11329/249>
- Dinauer, A., Mucci, A. 2017. Spatial variability in surface-water *p*CO₂ and gas exchange in the world's largest semi-enclosed estuarine system: St. Lawrence Estuary (Canada). *Biogeosciences* 14, 3221-3237, <https://doi.org/10.5194/bg-14-3221-2017>
- 635 Easley, R.A., Patsavas, M.C., Byrne, R.H., Liu, X., Feely, R.A., Mathis, J.T., 2013. Spectrophotometric measurement of calcium carbonate saturation states in seawater. *Environ. Sci. Technol.* 47 (3), 1468–1477.
- Elzhov, T.V., Mullen, K.M., Spiess, A.-N. Bolker, B., 2016. minpack.lm: R Interface to the Levenberg-Marquardt Nonlinear Least-Squares Algorithm Found in MINPACK, Plus Support for Bounds. R package version 1.2-1. <https://CRAN.R-project.org/package=minpack.lm>
- 640 Fong, M.B, Dickson, A.G. 2019. Insights from GO-SHIP hydrography data into the thermodynamic consistency of CO₂ system measurements in seawater. *Mar. Chem.* 211, 52-63, <https://doi.org/10.1016/j.marchem.2019.03.006>
- Gattuso, J.-P., Hansson, L. 2011. *Ocean Acidification*. Oxford: Oxford University Press.
- Gattuso, J.-P., Epitalon, J.-M., Lavigne, H., Orr, J. 2019. seacarb: Seawater Carbonate Chemistry. R package version 3.2.12. <https://CRAN.R-project.org/package=seacarb>
- 645 Goyet, C., Poisson, A. 1989. New determination of carbonic acid dissociation constants in seawater as a function of temperature and salinity. *Deep-Sea Res.* 36(11), 1635-1654, [https://doi.org/10.1016/0198-0149\(89\)90064-2](https://doi.org/10.1016/0198-0149(89)90064-2)
- Gray, A.R., Johnson, K.S., Bushinsky, S.M., Riser, S.C., Russell, J.L., Talley, L.D., Wanninkhof, R., Williams, N.L., Sarmiento, J.L. 2018. Autonomous Biogeochemical Floats Detect Significant Carbon Dioxide Outgassing in the High-Latitude Southern Ocean. *Geophys. Res. Lett.* 45, 9049-9057.
- 650 Gruber, N., Clement, D., Carter, B.R., Feely, R.A., van Heuven, S., Hoppema, M., Ishii, M., Key, R.M., Kozyr, A., Lauvset, S.K., Lo Monaco, C., Mathis, J.T., Murat, A., Olsen, A., Perez, F., Sabine, C.L., Tanhua, T., Wanninkhof, R. 2019. The oceanic sink for anthropogenic CO₂ from 1994 to 2007. *Science* 363(6432), 1193-1199.
- Hansson, I. 1973. A new set of acidity constants for carbonic acid and boric acid in sea water. *Deep-Sea Res.* 20, 461-478.
- Hunter, K.A. 1998. The temperature dependence of pH in surface seawater. *Deep-Sea Res. Pt. I* 45, 1919-1930.
- 655 Jansen, H., Wolf-Gladrow, D.A. 2001. Carbonate dissolution in copepod guts: a numerical model. *Mar. Ecol. Prog. Ser.* 221, 199-207.
- Johnson, K., Körtzinger, A., Mintrop, L., Duinker, J., Wallace, D., 1999. Coulometric total carbon dioxide analysis for marine studies: measurement and internal consistency of underway TCO₂ concentrations. *Mar. Chem.* 67 (1-2), 123–144.
- 660 Johnson, K.S., Plant, J.N., Coletti, L.J., Jannasch, H.W., Sakamoto, C.M., Riser, S.C., Swift, D.D., Williams, N.L., Boss, E., Haentjens, N., Talley, L.D., Sarmiento, J.L. 2017. Biogeochemical sensor performance in the SOCCOM profiling float array. *J. Geophys. Res.-Oceans* 122 (8), 6416-6436.
- Jutterström, S., Anderson, L.G. 2005. The saturation of calcite and aragonite in the Arctic Ocean. *Mar. Chem.* 94(1-4), 101-110. <https://doi.org/10.1016/j.marchem.2004.08.010>
- 665 Key, R.M., Olsen, A., van Heuven, S., Lauvset, S.K., Velo, A., Lin, X., Schirnick, C., Kozyr, A., Tanhua, T., Hoppema, M., Jutterström, S., Steinfeldt, R., Jeansson, E., Ishi, M., Perez, F.F., Suzuki, T. 2015. Global Ocean Data Analysis Project, Version 2 (GLODAPv2), ORNL/CDIAC-162, NDP-P093. Carbon Dioxide Information Analysis Center, Oak Ridge National Laboratory, US Department of Energy, Oak Ridge, Tennessee.
- Koeve, W., Oschlies, A. 2012. Potential impact of DOM accumulation on *f*CO₂ and carbonate ion computations in ocean acidification experiments. *Biogeosciences* 9(10), 3787-3798. doi:10.5194/bg-9-3787-2012



- 670 Landschützer, P., Gruber, N., Haumann, F.A., Rödenbeck, C., Bakker, D.C.E., Heuven, S.v., Hoppema, M., Metzl, N., Sweeney, C., Takahashi, T., Tilbrook, B., Wanninkhof, R. 2015. The reinvigoration of the Southern Ocean carbon sink. *Science* 349, 1221-1224.
- Lee, K., Kim, T.W., Byrne, R.H., Millero, F.J., Feely, R.A., Liu, Y.M., (2010). The universal ratio of boron to chlorinity for the North Pacific and North Atlantic oceans. *Geochimica Et Cosmochimica Acta* 74 (6), 1801-1811.
- 675 Le Quéré, C., Andrew, R.M., Friedlingstein, P., Sitch, S., Pongratz, J., Manning, A.C., Korsbakken, J.I., Peters, G.P., Canadell, J.G., Jackson, R.B., Boden, T.A., Tans, P.P., Andrews, O.D., Arora, V.K., Bakker, D.C.E., Barbero, L., Becker, M., Betts, R.A., Bopp, L., Chevallier, F., Chini, L.P., Ciais, P., Cosca, C.E., Cross, J., Currie, K., Gasser, T., Harris, I., Hauck, J., Haverd, V., Houghton, R.A., Hunt, C.W., Hurtt, G., Ilyina, T., Jain, A.K., Kato, E., Kautz, M., Keeling, R.F., Klein Goldewijk, K., Körtzinger, A., Landschützer, P., Lefèvre, N., Lenton, A., Lienert, S., Lima, I., Lombardozzi, D., Metzl, N., Millero, F.,
680 Monteiro, P.M.S., Munro, D.R., Nabel, J.E.M.S., Nakaoka, S.-i., Nojiri, Y., Padin, X.A., Pregon, A., Pfeil, B., Pierrot, D., Poulter, B., Rehder, G., Reimer, J., Rödenbeck, C., Schwinger, J., Séférian, R., Skjelvan, I., Stocker, B.D., Tian, H., Tilbrook, B., Tubiello, F.N., van der Laan-Luijkx, I.T., van der Werf, G.R., van Heuven, S., Viovy, N., Vuichard, N., Walker, A.P., Watson, A.J., Wiltshire, A.J., Zaehle, S., Zhu, D. 2018. Global Carbon Budget 2017. *Earth Syst. Sci. Data* 10, 405-448, <https://doi.org/10.5194/essd-10-405-2018>
- 685 Lewis, E., Wallace, D.W.R. 1998. Program Developed for CO₂ System Calculations, ORNL/CDIAC-105, Carbon Dioxide Inf. Anal. Cent., Oak Ridge Natl. Lab., Oak Ridge, Tenn., 38 pp..
- Lueker, T.J., Dickson, A.G., Keeling, C.D. 2000. Ocean *p*CO₂ calculated from dissolved inorganic carbon, alkalinity, and equations for *K*₁ and *K*₂: validation based on laboratory measurements of CO₂ in gas and seawater at equilibrium. *Mar. Chem.* 70(1-3), 105-119.
- 690 Lyman, J. 1956. Buffer Mechanism of Sea Water. (Ph.D. thesis), University of California, Los Angeles.
- Lyman, J. 1972. Development of Ideas concerning the Carbon Dioxide System in Sea Water up to 1940. *Proc. R. Soc. Edinb. B*, 72, 381-387.
- Mehrbach, C., Culberson, C.H., Hawley, J.E., Pytkowicz, R.M. 1973. Measurement of the apparent dissociation constants of carbonic acid in seawater at atmospheric pressure. *Limnol. Oceanogr.* 18(6), 897-907.
- 695 Millero, F.J. 1995. Thermodynamics of the carbon dioxide system in the oceans. *Geochim. Cosmochim. Ac.* 59(4), 661-677.
- Millero, F.J., Pierrot, D., Lee, K., Wanninkhof, R., Feely, R., Sabine, C.L., Key, R.M., Takahashi, T. 2002. Dissociation constants for carbonic acid determined from field measurements. *Deep-Sea Res. Pt. I*, 49, 1705-1723.
- Millero, F.J., Graham, T.B., Huang, F., Bustos-Serrano, H., Pierrot, D. 2006. Dissociation constants of carbonic acid in seawater as a function of salinity and temperature. *Mar. Chem.* 100(1-2), 80-94,
700 <https://doi.org/10.1016/j.marchem.2005.12.001>
- Millero, F.J. 2007. The Marine Inorganic Carbon Cycle. *Chem. Rev.* 107, 308-341
- Millero, F.J. 2010. Carbonate constants for estuarine waters. *Mar. Freshwater Res.* 61, 139-142
- Milliman, J.D., Troy, P.J., Balch, W.M., Adams, A.K., Li, Y.-H., Mackenzie, F.T. 1999. Biologically mediated dissolution of calcium carbonate above the chemical lysocline? *Deep-Sea Res. Pt. I* 46, 1653-1669.
- 705 Moberg, E.G., Greenber, D.M., Revelle, R., Allen, E.C. 1934. The buffer mechanism of sea water. *Bull. Scripps Instn Oceanogr. Tech. Ser.*, 3, 231-278.
- Morse, J.W., Mackenzie, F.T. 1990. *Geochemistry of Sedimentary Carbonates*. Elsevier, Amsterdam.
- Mucci, A. 1983. The solubility of calcite and aragonite in seawater at various salinities, temperatures and one atmosphere total pressure. *Am. J. Sci.* 283, 780-799, <http://doi.org/10.2475/ajs.283.7.780>
- 710 Naviaux, J.D., Subhas, A.V., Dong, S., Rollins, N.E., Liu, X., Byrne, R.H., Berelson, W.M., Adkins, J.F. Calcite dissolution rates in seawater: lab vs. in situ measurements and inhibition by organic matter. Under review in *Marine Chemistry*.



- Negrete-García, G., Lovenduski, N.S., Hauri, C., Krumhardt, K.M., Lauvset, S.K. 2019. Sudden emergence of a shallow aragonite saturation horizon in the Southern Ocean. *Nat. Clim. Change* 9, 313-317, <https://doi.org/10.1038/s41558-019-0418-8>
- 715 Olsen, A., Key, R.M., van Heuven, S., Lauvset, S.K., Velo, A., Lin, X., Schirnack, C., Kozyr, A., Tanhua, T., Hoppema, M., Jutterström, S., Steinfeldt, R., Jeansson, E., Ishii, M., Pérez, F.F., Suzuki, T. 2016. The Global Ocean Data Analysis Project version 2 (GLODAPv2) – an internally consistent data product for the world ocean. *Earth Syst. Sci. Data* 8, 297-323, <https://doi.org/10.5194/essd-8-297-2016>
- 720 Olsen, A., Lange, N., Key, R.M., Tanhua, T., Álvarez, M., Becker, S., Bittig, H.C., Carter, B.R., Cotrim da Cunha, L., Feely, R.A., van Heuven, S., Hoppema, M., Ishii, M., Jeansson, E., Jones, S.D., Jutterström, S., Karlsen, M.K., Kozyr, A., Lauvset, S.K., Lo Monaco, C., Murata, A., Pérez, F.F., Pfeil, B., Schirnack, C., Steinfeldt, R., Suzuki, T., Telszewski, M., Tilbrook, B., Velo, A., Wanninkhof, R. 2019 GLODAPv2.2019 – an update of GLODAPv2. *Earth Syst. Sci. Data* 113, 1437-1461. <https://doi.org/10.5194/essd-11-1437-2019>
- 725 Orr, J.C., Epitalon, J.-M., Dickson, A. G., Gattuso, J.-P. 2018. Routine uncertainty propagation for the marine carbon dioxide system. *Mar. Chem.* 207, 84-107, <https://doi.org/10.1016/j.marchem.2018.10.006>
- Palitzsch, S. 1923. Alkalinity and hydrogen ion concentration. *Int. Rev. Hydrobiol. Hydrogr.* 11, 398-437.
- Papadimitriou, S., Loucaides, S., Rérolle, V.M.C., Kennedy, P., Achterberg, E.P., Dickson, A.G., Mowlem, M., Kennedy, H. 2018. The stoichiometric dissociation constants of carbonic acid in seawater brines from 298 to 267 K. *Geochim. Cosmochim. Ac.* 220, 55-70, <https://doi.org/10.1016/j.gca.2017.09.037>
- 730 Patsavas, M.C., Byrne, R.H., Wanninkhof, R., Feely, R.A. and Cai, W.-J. 2015. Internal consistency of marine carbonate system measurements and assessments of aragonite saturation state: Insights from two U.S. coastal cruises. *Mar. Chem.* 176, 9–20.
- Pauling, L. 1970. *General Chemistry*, 3rd edition. New York: Dover Publications.
- Penry, D.L., Jumars, P.A. 1986 Chemical reactor analysis and optimal digestion. *BioScience* 36(5), 310-315.
- 735 Perez, F.F., Fraga, F. 1987. Association constant of fluoride and hydrogen ions in seawater. *Mar. Chem.* 21(2), 161-168.
- Pierrot, D., Lewis, E., Wallace, D.W.R. 2006. MS Excel Program Developed for CO₂ System Calculations, Tech. rep., Carbon Dioxide Inf. Anal. Cent., Oak Ridge Natl. Lab., US DOE, Oak Ridge, Tenn.
- Pierrot, D., Neill, C., Sullivan, K., Castle, R., Wanninkhof, R., Lüger, H., Johannessen, T., Olsen, A., Feely, R.A., Cosca, C.E. 2009. Recommendations for autonomous underway pCO₂ measuring systems and data-reduction routines. *Deep Sea Research Part II: Topical Studies in Oceanography* 56(8-10), 512-522., <https://doi.org/10.1016/j.dsr2.2008.12.005>
- 740 R Core Team. 2019. R: A language and environment for statistical computing. R Foundation for Statistical Computing, Vienna, Austria. URL <http://www.R-project.org/>.
- Raimondi, L., Matthews, J.B.R., Atamanchuck, D., Azetsu-Scott, K., Wallace, D. 2019. The internal consistency of the marine carbon dioxide system for high latitude shipboard and in situ monitoring. *Marine Chemistry*, in press, <https://doi.org/10.1016/j.marchem.2019.03.001>
- 745 Ribas-Ribas, M., Rérolle, V.M.C., Bakker, D.C.E., Kitidis, V., Lee, G.A., Brown, I., Achterberg, E.P., Hardman-Mountford, N.J., Tyrrell, T. 2014. Intercomparison of carbonate chemistry measurements on a cruise in northwestern European shelf seas. *Biogeosciences* 11, 4339-4355, <https://doi.org/10.5194/bg-11-4339-2014>
- Roy, R.N., Roy, L.N., Vogel, K.M., Porter-Moore, C., Pearson, T., Good, C.E., Millero, F.J., Campbell, D.M. 1993. The dissociation constants of carbonic acid in seawater at salinities 5 to 45 and temperatures 0 to 45°C. *Mar. Chem.* 44, 249-267.
- 750 Sharp, J.D., Byrne, R.H. 2019. Carbonate ion concentrations in seawater: Spectrophotometric determination at ambient temperatures and evaluation of propagated calculation uncertainties. *Mar. Chem.* 209, 70-80.



- Spiess, A.-N. 2018. propagate: Propagation of uncertainty using higher-order Taylor expansion and Monte Carlo simulation. R-package version 1.0-6. <https://CRAN.R-project.org/package=propagate>
- 755 Soetaert K., Herman, P.M.J., 2009. A Practical Guide to Ecological Modelling. Using R as a Simulation Platform. Springer, 372 pp.
- Stumm, W., Morgan, J.J. 1996. Aquatic Chemistry: Chemical Equilibria and Rates in Natural Waters, 3rd Edition (Vol. 105). New York: John Wiley & Sons.
- Takahashi, T., Sweeney, C., Hales, B., Chipman, D., Newberger, T., Goddard, J., Iannuzzi R., Sutherland, S. 2012. The Changing Carbon Cycle in the Southern Ocean. *Oceanography* 25(3), 26-37.
- 760 Takeshita, Y., Johnson, K.S., Martz, T.R., Plant, J.N., Sarmiento, J.L. 2018. Assessment of Autonomous pH Measurements for Determining Surface Seawater Partial Pressure of CO₂. *J. Geophys. Res.-Oceans* 123, 4003-4013.
- Tanhua, T., Van Heuven, S., Key, R.M., Velo, A., Olsen, A., Schirnick, C. 2010. Quality control procedures and methods of the CARINA database, *Earth Syst. Sci. Data* 2, 205-240, <https://doi.org/10.5194/essd-2-35-2010>
- 765 Tishchenko, P.Y., Wong, C.S., Johnson, W.K. 2013. Measurements of Dissociation Constants of Carbonic Acid in Synthetic Seawater by Means of a Cell Without Liquid Junction. *J. Solution Chem.* 42(11), 2168-2186, <https://doi.org/10.1007/s10953-013-0094-7>
- Uppström, L.R. 1974. The boron/chlorinity ratio of deep-sea water from the Pacific Ocean. *Deep-Sea Res. Oceanogr. Abstr.* 21, 161-162.
- 770 van Heuven, S., Pierrot, D., Rae, J.W.B., Lewis, E., Wallace, D.W.R. 2011. MATLAB program developed for CO₂ system calculations, ORNL/CDIAC-105b, Carbon Dioxide Inf. Anal. Cent., Oak Ridge Natl. Lab., US DOE, Oak Ridge, Tenn.
- Wanninkhof, R., Lewis, E., Feely, R., Millero, F., 1999. The optimal carbonate dissociation constants for determining surface water pCO₂ from alkalinity and total inorganic carbon. *Mar. Chem.* 65 (3–4), 291–301.
- Weiss, R. 1974. Carbon dioxide in water and seawater: the solubility of a non-ideal gas. *Mar. Chem.* 2(3), 203-215.
- 775 Williams, N.L., Juraneck, L.W., Feely, R.A., Johnson, K.S., Sarmiento, J.L., Talley, L.D., Dickson, A.G., Gray, A.R., Wanninkhof, R., Russell, J.L., Riser, S.C. and Takeshita, Y. 2017. Calculating surface ocean pCO₂ from biogeochemical Argo floats equipped with pH: An uncertainty analysis. *Global Biogeochem. Cy.* 31, 591-604.
- Yang, B., Byrne, R.H. and Lindemuth, M. 2015. Contributions of organic alkalinity to total alkalinity in coastal waters: A spectrophotometric approach. *Mar. Chem.* 176, 199–207.
- 780 Yao, W., Millero, F.J. 1996. Oxidation of hydrogen sulfide by hydrous Fe (III) oxides in seawater. *Mar. Chem.* 52(1), 1-16.
- Zeebe, R.E., Wolf-Gladrow, D. 2001. CO₂ in seawater: equilibrium, kinetics, isotopes. Amsterdam: Elsevier Science.

785